Chemistry & Biology
Article

A Semisynthetic Eph Receptor Tyrosine Kinase Provides Insight into Ligand-Induced Kinase Activation

Nikhil Singla,[1,2] Hediye Erdjument-Bromage,[3] Juha P. Himanen,[1] Tom W. Muir,[2,4] and Dimitar B. Nikolov[1,2,*]
[1]Structural Biology Program, Memorial Sloan-Kettering Cancer Center, New York, NY 10065, USA
[2]Tri-Institutional Chemical Biology Program, Weill Cornell Medical College, New York, NY 10065, USA
[3]Molecular Biology Program, Memorial Sloan-Kettering Cancer Center, New York, NY 10065, USA
[4]Laboratory of Synthetic Protein Chemistry, The Rockefeller University, New York, NY 10065, USA
*Correspondence: nikolovd@mskcc.org
DOI 10.1016/j.chembiol.2011.01.011

SUMMARY

We have developed a methodology for generating milligram amounts of functional Eph tyrosine kinase receptor using the protein engineering approach of expressed protein ligation. Stimulation with ligand induces efficient autophosphorylation of the semisynthetic Eph construct. The in vitro phosphorylation of key Eph tyrosine residues upon ligand-induced activation was monitored via time-resolved, quantitative phosphoproteomics, suggesting a precise and unique order of phosphorylation of the Eph tyrosines in the kinase activation process. To our knowledge, this work represents the first reported semisynthesis of a receptor tyrosine kinase and provides a potentially general method for producing single-pass membrane proteins for structural and biochemical characterization.

INTRODUCTION

Receptor tyrosine kinases (RTKs) control numerous cellular signaling pathways that regulate the fundamental processes of cell migration, proliferation, differentiation, and metabolism (Hubbard and Till, 2000; Schlessinger, 2000). As type I transmembrane proteins, RTKs consist of an extracellular region, a transmembrane helix and an intracellular region that contains a tyrosine kinase catalytic domain. RTKs have the unique capacity to transduce the extracellular signal generated on binding to their cognate ligands, to the cytoplasm by phosphorylating tyrosine residues on the receptors themselves and on downstream signaling proteins. Despite the progress over the past several years in elucidating the molecular details of RTK signaling in regulating crucial physiological processes, the fundamental question persists, how is ligand engagement outside the cell coupled to kinase activation within the cell? A major impediment in conducting functional and structural studies in vitro is the lack of efficient recombinant protein expression systems to produce large amounts of purified transmembrane protein (Drew et al., 2003). Thus, although one third of our genome codes for integral membrane proteins (Wallin and von Heijne, 1998), relatively little information is available about their three-dimensional structures and mechanisms. While there have been some important advances in producing multipass transmembrane proteins (Jiang et al., 2003; Kawate and Gouaux, 2006), production of full-length RTKs in sufficient quantities for biophysical and structural characterization still remains a major experimental challenge. This is partially due to the fact that the majority of the multipass transmembrane protein domains are embedded in the membrane and can therefore be subjected to much harsher conditions and also efficiently refolded if necessary. On the other hand, RTKs only have a single-pass helix embedded in the membrane, while their disulfide-bonded extracellular region normally resides in an oxidizing environment, whereas the intracellular region consisting of the catalytic kinase domain resides in a reducing environment. Indeed, these modular domains can usually be expressed easily and studied as soluble fragments individually, using suitable recombinant expression systems, but not together in a full-length receptor. Thus, our work in this report is focused on producing full-length Eph RTK for elucidating the molecular steps in receptor activation.

We focused on the largest family of RTKs, the Eph receptors, which, together with their membrane-anchored ephrin ligands, initiate unique bidirectional signaling cascades at sites of cell-cell contact (Chumley et al., 2007; Kullander and Klein, 2002; Lackmann and Boyd, 2008; Pasquale, 2005). These signals regulate cell migration, tissue patterning, axon guidance, development of the nervous and the vascular system, learning and memory, glucose homeostasis, immunological and inflammatory host responses, bone maintenance and remodeling, and in the development and metastasis of many tumors. The Eph receptors and ephrin ligands are divided into two subclasses, A and B, based on sequence homology and their binding affinities for each other (Eph Nomenclature Committee, 1997). In general, the A-subclass Eph receptors (EphA1-A10) bind to the A-subclass ephrins (ephrin-A1-A6), and the B-subclass Eph receptors (EphB1-B6) interact with the B-subclass ephrins (ephrin-B1-B3) (Himanen et al., 2007). Like other type I RTKs, the Eph receptors comprise of an N-terminal disulfide-bonded, glycosylated ectodomain, which consists of a ligand-binding domain and an adjacent cysteine rich region followed by two fibronectin type III repeats. A single transmembrane helix separates the ectodomain from the intracellular region, which consists of a juxtamembrane segment, a tyrosine kinase domain

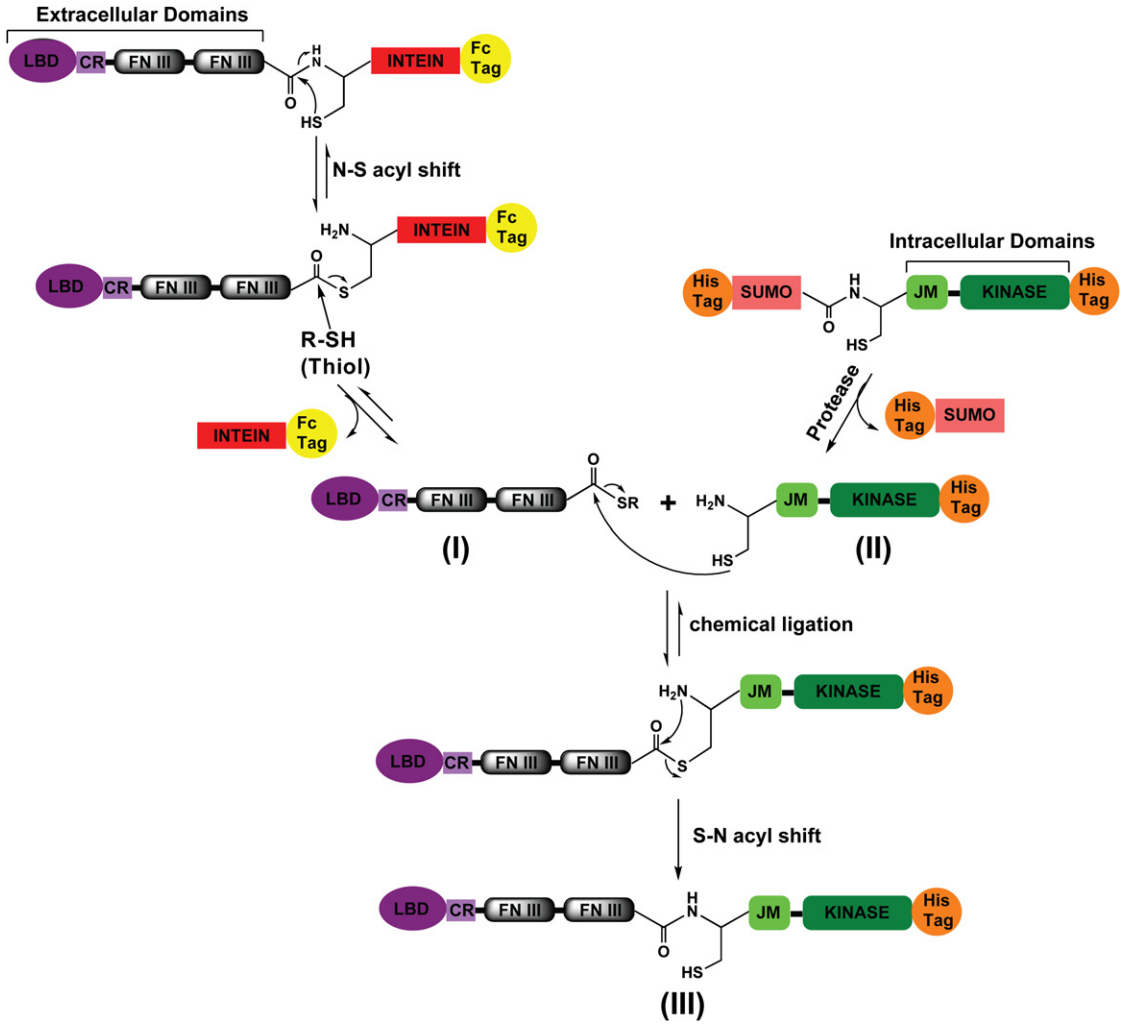

Figure 1. Summary of the EPL Strategy

Intein-mediated thiolysis generates the Eph ECD α-thioester (I) (LBD: ligand binding domain, CR: cysteine rich region, FN III: fibronectin type III repeat). The intein-Fc-purification-tag fragment is separated by affinity chromatography. Protease treatment cleaves the SUMO fusion protein with histidine (His) purification tag and unmasks the cysteine residue at the N terminus of the Eph ICD (II) (JM: juxtamembrane region, Kinase: tyrosine kinase domain; His: purification tag). The two reactive building blocks I and II are chemically ligated to generate the semisynthetic Eph RTK sans the transmembrane helix (III). See also Figures S1 and S2.

and a sterile-α motif (SAM) domain often linked to a C-terminal PDZ-binding motif. The Eph RTK serve as a good model system for understanding the general biochemical and structural details of RTK activation.

Cell-based expression systems, both in cells that endogenously express the Eph protein and also genetically engineered cell lines, have failed to produce high levels of the pure full-length Eph receptor (Boyd et al., 1992; Dottori et al., 1999; Lawrenson et al., 2002; Mizushima and Nagata, 1990). Our work presented here is aimed at overcoming this problem by using a novel chemical biology approach, namely expressing the functional Eph intracellular and extracellular regions separately in different expression systems and joining them in vitro using expressed protein ligation (EPL) (Muir, 2003; Muir et al., 1998). EPL is an extension of native chemical ligation (Dawson et al., 1994) where the reacting protein fragments contain either a N-terminal cysteine or a C-terminal α-thioester, for the semisynthesis of a target protein (Muralidharan and Muir, 2006). We recently described the utilization of the EPL protein semisynthesis approach to selectively modify glycosylated and disulfide-bonded Eph ectodomains secreted from eukaryotic cell lines (Singla et al., 2008). Here, we present further development of this method to reconstitute an Eph RTK sans the transmembrane region and use the generated semisynthetic protein to gain insight into the mechanism of ligand-induced kinase activation.

RESULTS

Generating Semisynthetic Eph RTK

Our semisynthetic strategy required the generation of an α-thioester derivative of the recombinant Eph extracellular domains (ECD), which can then be ligated to the recombinant intracellular domains (ICD) containing a cysteine at the N terminus (Figure 1). The complete EphA4 ECD, which consists of an

ephrin-binding domain, an adjacent cysteine rich region followed by two fibronectin type III repeats, was fused to an engineered version of the *Mycobacterium xenopi* GyrA intein and a Fc purification tag. C-terminal intein fusions can be used to directly introduce α-thioester groups into recombinant proteins through a thiolysis cleavage reaction (Severinov and Muir, 1998). The fusion construct was expressed as a secreted protein in insect-cells and was purified from the cell media by affinity chromatography on Protein-A Sepharose using the Fc tag. Thiolysis of the intein fusion to introduce the α-thioester in the EphA4 ECD was initiated with 2-mercaptoethanesulfonic acid (MESNA) as described previously (Singla et al., 2008). Structural studies of the Eph and ephrin interaction domains have shown that complex formation takes place via an extensive interaction interface and that the disulfide bonds on the extracellular domains of both receptor and ligand are essential for their correct folding and complex formation (Himanen et al., 2001). Hence, the biological activity of the EphA4 ECD α-thioester (obtained after thiol treatment) in forming specific high-affinity complexes with its respective ephrin ligand was established using pull-down and size exclusion chromatography (SEC) binding assays (see Figures S1A and S1B available online).

The Eph (EphA3 or EphA4) ICD, including the juxtamembrane and the kinase domains, was expressed as a fusion to the small ubiquitin-like modifier (SUMO) in *Escherichia coli,* with histidine tags included to allow for immobilized metal ion affinity purification. SUMO is an 11 kDa protein that covalently attaches to specific target proteins leading to changes in their function and activity (Muller et al., 2001; Saitoh et al., 1997). While various other fusion constructs were tested for recombinant expression of Eph ICD, the fusion with SUMO, which is known to increase the expression and solubility of recombinant proteins (Butt et al., 2005; Marblestone et al., 2006), resulted in the highest yields. Treatment with ubiquitin-like protein processing enzyme, SUMO protease, which specifically cleaves conjugated SUMO from target proteins by recognizing its tertiary structure (Li and Hochstrasser, 1999; Mossessova and Lima, 2000), leaves a serine residue at the N terminus of the Eph ICD. As a requisite for the ligation chemistry, a site directed serine to cysteine mutation was introduced at the N terminus of the Eph ICD; this was well tolerated and affected neither the expression levels of the fusion protein nor the protease cleavage efficiency. An important consideration while designing the semisynthesis reaction is that the cysteine residue at the ligation junction should be derived from the native sequence of the protein if possible; otherwise a conservative mutation should be introduced in a residue that is not crucial for the function of the protein (Muralidharan and Muir, 2006; Schwarzer and Cole, 2005). The cysteine residue at the ligation junction in our constructs corresponds to cysteine 568 in the native EphA3 ICD sequence, and is a serine 574 to cysteine mutation in case of the EphA4 ICD. The fusion proteins were treated with SUMO protease, which unmasked the cysteine residue at the N terminus of the respective Eph ICD. The cleavage efficiency within 30 min was approximately 90% (Figure S2A). The SEC profile of the Eph ICD obtained after cleavage confirmed that it was properly folded and monomeric (Figure S2B). The efficient and fast cleavage generated high amounts of reactive Eph ICD and its viability for EPL reaction was confirmed by ligation with a synthetic peptide α-thioester (Figure S2C).

Having produced the two recombinant protein building blocks, the ligation reaction between the EphA4 ECD α-thioester and the ICD containing a cysteine residue in its N terminus was performed in the presence of tris(2-carboxyethyl)phosphine (TCEP) and MESNA, to suppress any competing and unproductive oxidation and hydrolysis reactions (Dawson et al., 1994; Muralidharan and Muir, 2006). The concentrations of these reagents were experimentally adjusted such that they did not reduce the buried disulfide bonds in the Eph ECD (Himanen et al., 2001, 2010). The ligation product was partially purified by SEC, with the only impurity derived from the unligated EphA4 ECD α-thioester (Figure 2A). The unligated EphA4 ICD (Mw ~36 kDa) elutes separately but the unligated EphA4 ECD α-thioester (Mw ~60 kDa) partially coelutes with the semisynthetic EphA4 receptor (Mw ~96 kDa). Therefore, peak fractions corresponding to the semisynthetic EphA4 receptor and the unligated EphA4 ECD α-thioester were pooled and a final purification was performed using Ni^{2+} affinity chromatography via the histidine tag at the C terminus of the semisynthetic EphA4 receptor (Figure 2B). The purified semisynthetic product was subjected to SEC and resolved on SDS-PAGE revealing lack of significant impurities (Figure 2C). The SEC profile of the purified semisynthetic Eph receptor also confirmed that it is monomeric in solution. Similarly, using the reactive EphA4 ECD α-thioester and the reactive EphA3 ICD, a chimeric (EphA4ECD-EphA3ICD) semisynthetic protein was also generated (Figures S3A–S3C). The production yield for the EphA4 ECD fusion protein (EphA4ECD-intein-Fc) is ~20 mg per liter of cell culture and the cleavage efficiency (with 50 mM MESNA) to generate the reactive EphA4 ECD α-thioester is approximately 40% (i.e., ~8 mg/liter). The yield for the EphA3 and EphA4 ICD fusion proteins (His-SUMO-EphA3/A4ICD-His) is ~15 and ~12 mg/liter, respectively. The cleavage efficiency with the SUMO protease to unmask the N-terminal cysteine residue and generate the reactive EphA3 and EphA4 ICD proteins is approximately 90%. The chemical ligation yield upon mixing the two reactive Eph building blocks (in a 1:1 ratio) is approximately 50%. Thus, we obtain approximately 4 mg of the pure, homogenous semisynthetic Eph receptor from a liter of Eph ECD expression media and 1/2 l of Eph ICD expression media.

The Semisynthetic Eph RTK Retains the Biological Activity of Its Individual Domains

Upon optimization of the protocol for production of multimilligram amounts of pure semisynthetic Eph receptor, we confirmed that the individual protein domains maintained their native biological activity after the chemical ligation reaction. For the EphA4 ECD in the semisynthetic receptor, a pull-down binding assay was performed with ephrin ligand (Figure 3A). The formation of specific, high-affinity complex with Fc-tagged ephrin-A5 (ephrin-A5-Fc) confirmed that the EphA4 ECD in the semisynthetic protein maintained its correct fold, disulfide-bond pattern, and ligand binding properties. For the intracellular tyrosine kinase domain, an enzyme-linked immunosorbent assay (ELISA)-based kinase assay was performed using a synthetic poly-Glu-Tyr substrate peptide (Figure 3B). The assay documented that the Eph kinase domain, maintains a similar

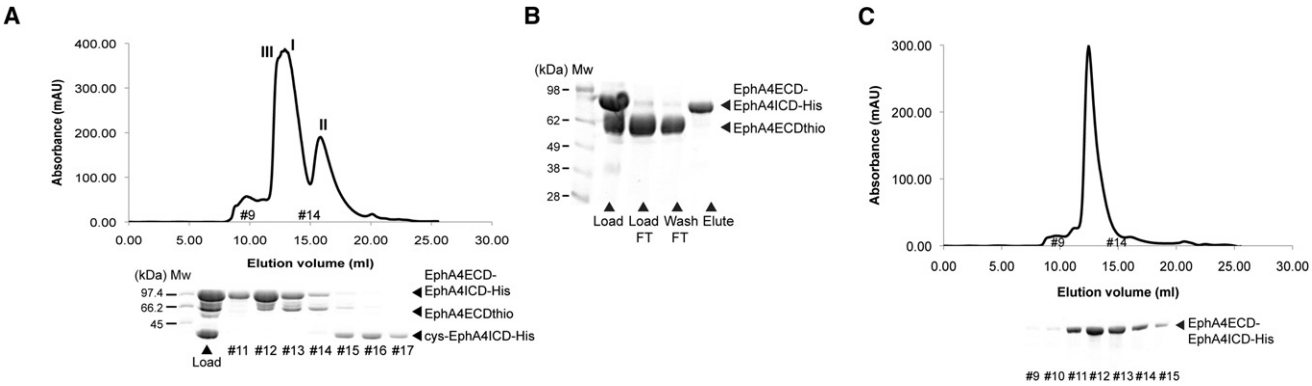

Figure 2. Semisynthesis of Eph RTK

(A) SEC (size exclusion chromatography) characterization of the products of the chemical ligation reaction. The major peaks I, II, and III correspond to the EphA4 ECD α-thioester (EphA4ECDthio), EphA4 ICD (cys-EphA4ICD-His), and the semisynthetic EphA4 receptor (EphA4ECD-EphA4ICD-His), respectively. An aliquot of the sample loaded on the SEC column (load) and the fractions under the corresponding peaks are resolved by SDS-PAGE. All shown SDS-PAGEs are Coomassie stained. (Mw) Molecular weight marker (in kilodaltons).

(B) SDS-PAGE analysis of the semisynthetic EphA4 receptor purification. Fractions corresponding to peaks I and III were loaded on an immobilized metal ion affinity column (load). The unligated EphA4ECDthio impurity (lacking a histidine tag) is collected in the flow through (load FT) and the wash step (wash FT). Only the semisynthetic EphA4ECD-EphA4ICD-His protein binds to the column, which is then eluted (elute).

(C) SEC profile for the eluted protein from the affinity column. The fractions under the major peak are resolved on SDS-PAGE and correspond to >95% pure semisynthetic EphA4 receptor.

See also Figure S3.

enzymatic profile in transphosphorylating a substrate before and after ligation. To further characterize the enzymatic properties of the Eph kinase domain, its affinity for a synthetic biotinylated poly-Glu-Tyr peptide and ATP substrates was also evaluated using ELISA. The K_m values for ATP (Figure 3C) and for the peptide substrate (Figure S4) of the EphA3 kinase domain before and after ligation were comparable, suggesting that the Eph ICD retains its enzymatic activity after the chemical ligation reaction. Since, the EphA4 and EphA3 kinase domains are autophosphorylated during overexpression, we also performed a western blot evaluation of the phosphorylation state of the respective semisynthetic Eph receptors using phosphotyrosine antibody in the presence and absence of the *Yersinia* phosphotyrosine protein phosphatase (YOP) (Black and Bliska, 1997; Guan and Dixon, 1990), which has high specificity for phosphotyrosines and broad substrate protein recognition (Zhang et al., 1992) (Figure 3D). This analysis revealed that (1) phosphorylated tyrosine residues in the semisynthetic Eph receptor can be specifically recognized by phosphotyrosine antibodies; (2) using phosphatases we can dephosphorylate the protein; and (3) we can follow the enzymatic activity of the Eph tyrosine kinase domain resulting in its autophosphorylation in the presence of phosphatase inhibitors, ATP and Mg^{2+}. The activity of the kinase domain of the semisynthetic Eph receptor in transphosphorylating a peptide substrate both before and after treatment with phosphatase, was also evaluated using ELISA (Figure 3E). The reaction with the phosphatase-treated kinase sample was slower, presumably because autophosphorylation was required before the substrate peptide could be phosphorylated. These experiments confirmed that both the autophosphorylation activity of the tyrosine kinase domain and its ability to efficiently transphosphorylate other substrates were maintained in the semisynthetic Eph receptors.

Ligand-Induced Autophosphorylation of the Semisynthetic Eph RTK

We next sought to monitor in vitro the ligand-induced activation of the generated semisynthetic Ephs. Specifically, we examined the autophosphorylation of the tyrosine kinase domain in the semisynthetic Eph receptors upon addition of the ephrin ligand in different oligomeric states using two distinct approaches: a radioactivity-based assay and mass spectrometry. While the Fc-tagged ephrin (ephrin-Fc) ligand forms dimers that can induce the formation of active Eph-ephrin tetramers, sufficient for basal Eph kinase phosphorylation (Himanen and Nikolov, 2003), it has been shown that effective Eph activation under physiological conditions in vivo requires the multimerization (clustering) of the Eph/ephrin complexes, which can be achieved by preclustering of ephrin-Fc with anti-Fc antibodies (Davis et al., 1994) (Figure S5A). Hence, the semisynthetic Eph receptor was incubated with either preclustered or dimeric ephrin-A5-Fc. The western blot analysis earlier in Figure 3D had shown that the kinase domain in the semisynthetic Eph receptor is phosphorylated. Therefore, the Eph-ephrin complexes were first incubated with phosphatase, and then with phosphatase inhibitors. The first step dephosphorylated the semisynthetic Eph protein and the second step inactivated the phosphatase so that we could follow the phosphorylation upon addition of ATP and Mg^{2+}. For the radioactivity-based assays, [γ^{32}-P] ATP was added to the above samples and the autophosphorylation of the kinase was followed over a period of time. The stimulation of EphA4 receptor autophosphorylation by preclustered ephrin-A5-Fc was more efficient than that by dimeric ephrin-A5-Fc, while it was much slower in the absence of ephrin ligand (Figure 4A). We also quantified the incorporation of phosphate in these experiments (Figure S5B). The stoichiometry of the phosphorylated sites in the semisynthetic EphA4 receptor in

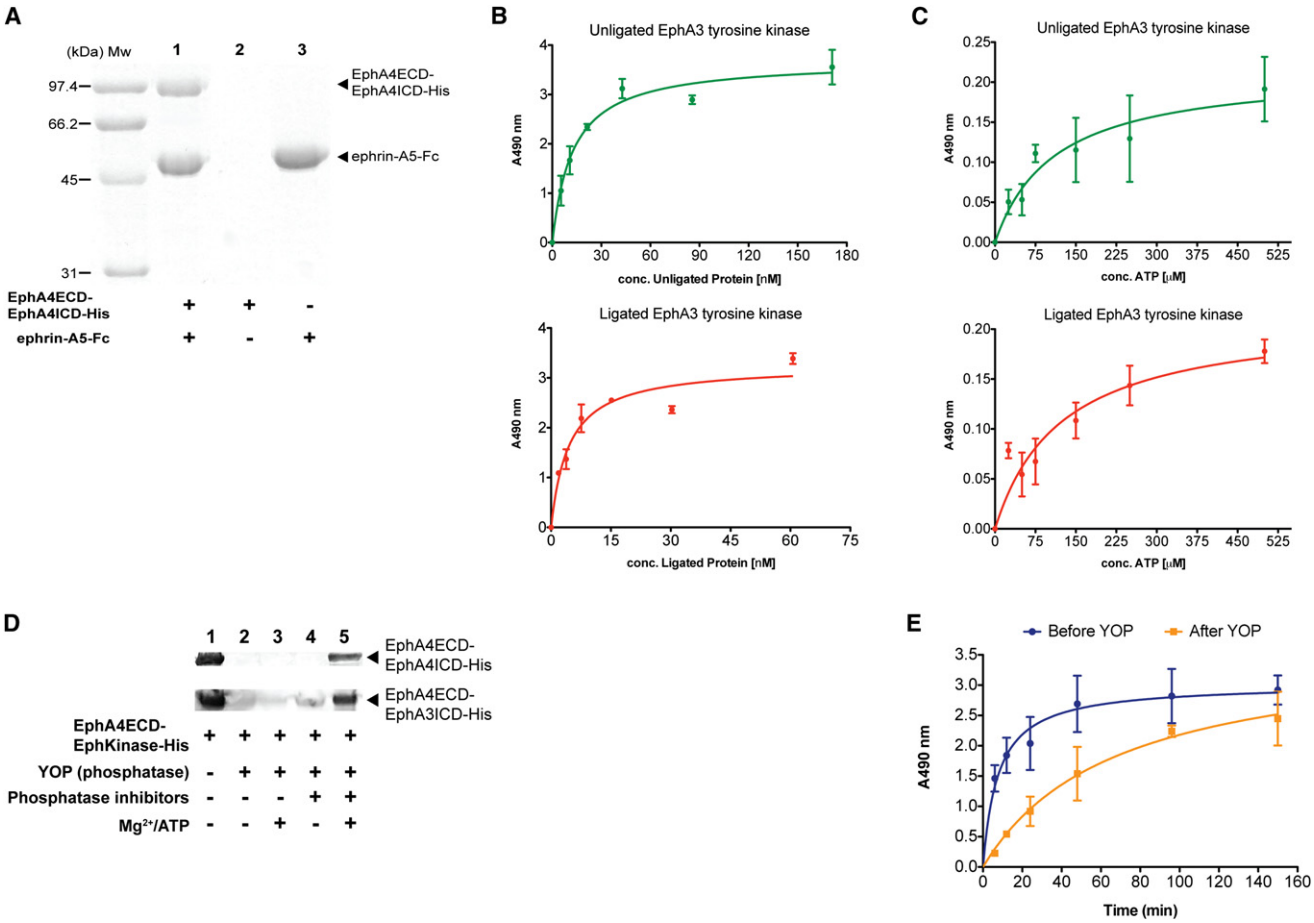

Figure 3. Both the ECD and the ICD Retain Full Biological Activity in the Semisynthetic Eph Receptor

(A) The semisynthetic Eph receptor (EphA4ECD-EphA4ICD-His) forms a specific complex with the Fc-tagged ephrin-A5 ligand (ephrin-A5-Fc), which can be pulled-down by Protein-A Sepharose beads (lane 1). The semisynthetic protein by itself does not bind to the beads (lane 2) whereas the binding of ephrin-A5-Fc alone to the beads is shown (lane 3). The SDS-PAGE is Coomassie stained. (Mw) Molecular weight marker (in kilodaltons).

(B) Representative plots for the phosphorylation of peptide substrate at different concentration of the unligated (His-SUMO-EphA3ICD-His) (top panel) and ligated (EphA4ECD-EphA3ICD-His) (lower panel) EphA3 ICD using an ELISA-based assay.

(C) Affinity for ATP of the EphA3 tyrosine kinase. Phosphorylation of a biotinylated peptide substrate by the unligated (His-SUMO-EphA3ICD-His) (top panel) and ligated (EphA4ECD-EphA3ICD-His) (lower panel) EphA3 ICD was monitored at different concentrations of ATP using an ELISA-based assay. The K_m values for ATP were 110.6 ± 46.9 and 122.8 ± 42.9 μM for the unligated and ligated EphA3 ICD, respectively, comparable to previously reported values (Davis et al., 2008).

(D) Western blot analysis for the semisynthetic Eph protein with EphA4 (EphA4ECD-EphA4ICD-His) (top panel) and EphA3 (EphA4ECD-EphA3ICD-His) (lower panel) ICD using phosphotyrosine antibody. The semisynthetic proteins are autophosphorylated (lane 1); Treatment with YOP phosphatase dephosphorylates them (lane 2) and the proteins are not autophosphorylated back upon addition of either Mg^{2+}/ATP (lane 3) or phosphatase inhibitors (lane 4) individually. Simultaneous incubation of the dephosphorylated proteins with phosphatase inhibitors and Mg^{2+}/ATP results in autophosphorylation of the semisynthetic Eph proteins (lane 5).

(E) Progress curves for the transphosphorylation of peptide substrate by semisynthetic Eph protein (EphA4ECD-EphA3ICD-His), before (blue) and after (orange) phosphatase treatment using the ELISA-based assay. Error bars represent the SD of three independent reactions.

See also Figure S4.

the presence of dimeric and preclustered ephrin-A5-Fc ligand at the 1800 s time point was ~4.0 mol of phosphate/mol of semisynthetic protein. To further confirm that we were observing ligand-induced increase in Eph autophosphorylation, we repeated the experiments, in the presence of a peptide Eph antagonist (K-Y-L-P-Y-W-P-V-L-S-S-L) that selectively inhibits ligand binding and ephrin-induced autophosphorylation of EphA4 in vivo (Murai et al., 2003). The boost in the ephrin-induced autophosphorylation of the semisynthetic Eph receptor was lost when preincubated with the inhibitor, making it similar to that observed in the absence of ligand (Figure 4B). These experiments established that we could follow the enzymatic activity of the kinase domain of our semisynthetic Eph receptor in response to ephrin binding to its extracellular region.

Monitoring the Phosphorylation of Individual Tyrosines in the Semisynthetic Eph RTK

To investigate the phosphorylation of individual Eph tyrosine residues in the semisynthetic receptor in response to ephrin-induced activation, we next applied label-free relative quantification by

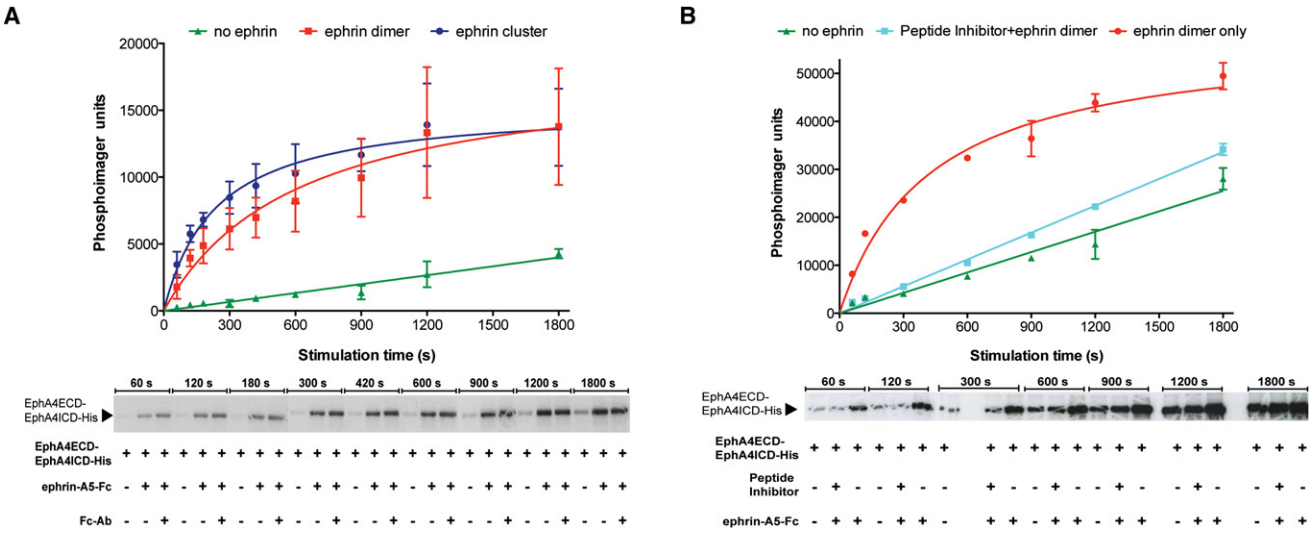

Figure 4. Kinase Domain Activation in the Semisynthetic Eph Receptor after Stimulation with Ephrin Ligand

(A) Autoradiograph for monitoring the semisynthetic EphA4 receptor (EphA4ECD-EphA4ICD-His) autophosphorylation over a period of time alone or in complex with dimeric (ephrin-A5-Fc) and preclustered (ephrin-A5-Fc + anti-Fc antibody, *Fc-Ab*) ephrin ligand. Progress curves were plotted for EphA4 by itself (green), in complex with dimeric (red) and preclustered (blue) ephrin ligand as quantified using a PhosphorImager.

(B) Loss of ligand-induced autophosphorylation of the semisynthetic Eph receptor in presence of peptide inhibitor. Autoradiograph for monitoring the semisynthetic EphA4 receptor (EphA4ECD-EphA4ICD-His) autophosphorylation over a period of time alone or in complex with dimeric (ephrin-A5-Fc) ephrin ligand in the presence and absence of a peptide Eph antagonist. Progress curves were plotted for EphA4 by itself (green) and in complex with dimeric ephrin ligand with (cyan) and without (red) preincubation with the peptide inhibitor as quantified using a PhosphorImager. Error bars represent the SD of three independent reactions. See also Figure S5.

mass spectrometry analysis using nano-LC-MS/MS. We focused on important individual tyrosine residues that have been implicated in regulating the catalytic activity of the Eph kinase domain (Binns et al., 2000; Davis et al., 2008; Wiesner et al., 2006; Wybenga-Groot et al., 2001). In the case of EphA4, the phosphorylation of the two-juxtamembrane tyrosine residues, Y_{596} (Y_{JM1}) and Y_{602} (Y_{JM2}), and of the conserved tyrosine in the kinase activation loop, Y_{779} (Y_{act}), play the most important roles in the activation of the receptor. Hence, these three residues were monitored in time-resolved phosphoproteomics experiments in the uncomplexed EphA4, and upon binding of dimeric and preclustered ephrin-A5-Fc (Figure S6A). Tandem mass spectra (MS/MS) corresponding to the tryptic peptides containing the phosphorylated juxtamembrane tyrosine residues Y_{JM1} and Y_{JM2}, and the activation loop tyrosine Y_{act} were identified (Figure S6B). Spectral (MS/MS) counts associated with individual phosphorylation of Y_{JM1} and Y_{JM2}, respectively, and for their joint ($Y_{JM1+JM2}$, double) phosphorylation are shown in Figure 5A. The data reveal that phosphorylation of Y_{JM1} alone is minimal over the time course of the experiment for all the samples. Significant phosphorylation of Y_{JM1} is only observed after Y_{JM2} is substantially phosphorylated upon stimulation with ephrin ligand. As both the juxtamembrane loop tyrosine residues of the semisynthetic EphA4 receptor are present on the same tryptic peptide, the spectral (MS/MS) counts for their autophosphorylation individually and jointly were summed ($Y_{JM1(Total)} = Y_{JM1} + Y_{JM1+JM2}$ and $Y_{JM2(Total)} = Y_{JM2} + Y_{JM1+JM2}$) to visualize better the total-autophosphorylation time courses of these tyrosines ($Y_{JM1(Total)}$ and $Y_{JM2(Total)}$) upon activation with preclustered ephrin-A5-Fc (Figure S7). Analysis of the spectral counts associated with Y_{act} (Figure 5B) showed that its phosphorylation increased as the reaction progressed over time and the increase was most significant after both Y_{JM1} and Y_{JM2} became phosphorylated.

To confirm the critical importance of Y_{JM2} in the kinase activation process as observed in our mass spectrometry experiments, and as suggested in earlier reports (Binns et al., 2000; Wybenga-Groot et al., 2001), we used site-directed mutagenesis. The ligand-induced kinase autophosphorylation of semisynthetic wild-type EphA4 and EphA4 with phenylalanine substitutions of the juxtamembrane tyrosines was measured with the radioactivity-based assays (Figure 5C). Significant loss in the autophosphorylation activity, as compared to the wild-type protein, was observed when Y_{JM2} was mutated, but not when Y_{JM1} alone was substituted.

DISCUSSION

EPL has been previously used to modify intracellular and multipass transmembrane proteins that can be folded to the native state after the chemical ligation reaction (Valiyaveetil et al., 2002), but its application to RTKs with large multidomain extracellular and intracellular regions normally residing in different redox environments, has not been documented. We now report the development of this semisynthetic technique to reconstitute an Eph RTK where all functional domains fully retain their biological activity. The production of multimilligram amounts of pure and monodisperse semisynthetic Eph receptors, made possible by this technology, provide a unique opportunity for their structural and mechanistic analysis in vitro to answer fundamental questions regarding their molecular mechanism of action. In

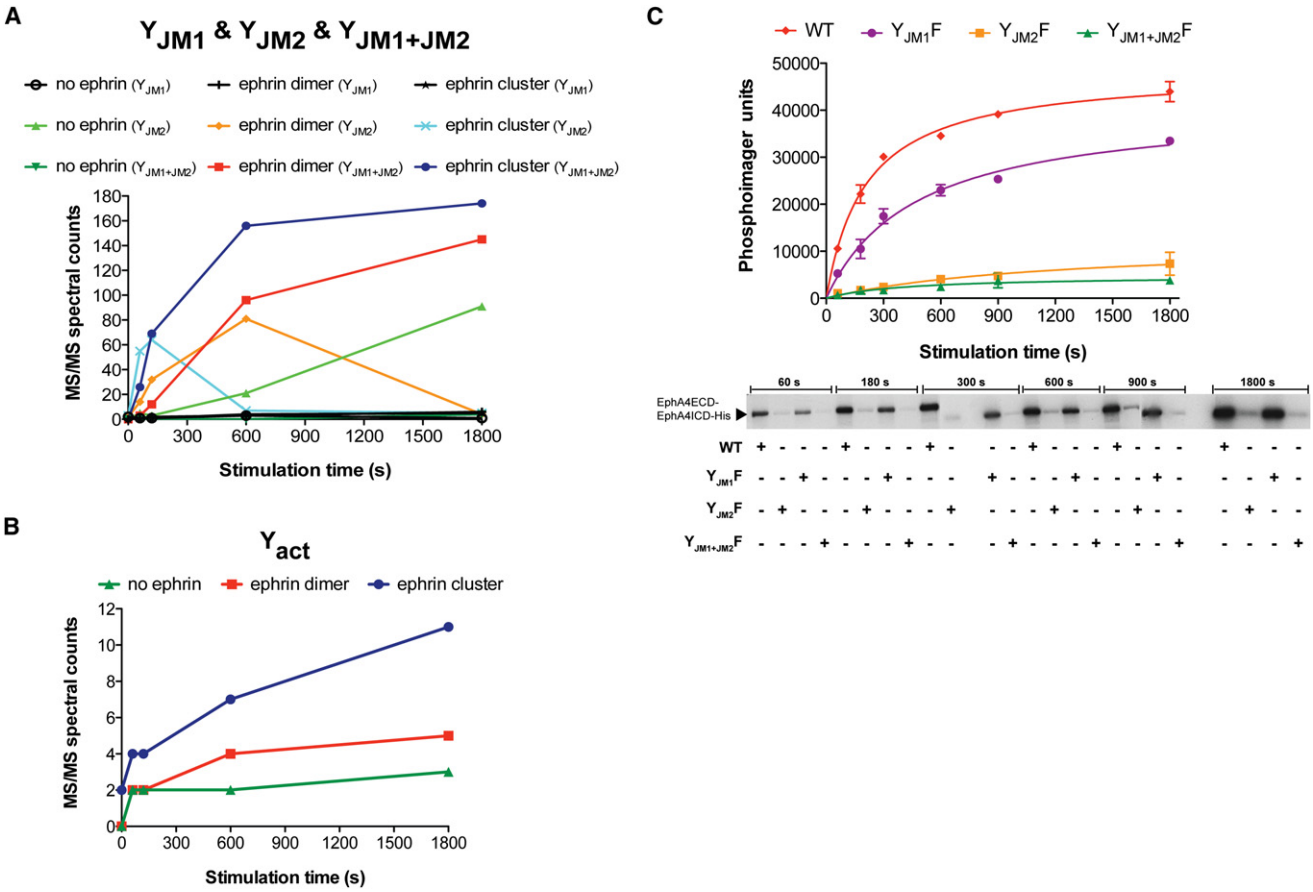

Figure 5. Analysis of the Phosphorylation Time Courses Of Individual Tyrosine Residues in the Semisynthetic Eph Receptor after Stimulation with Ephrin

(A) Phosphoproteomics analysis. The phosphorylation levels of the semisynthetic receptor juxtamembrane loop tyrosine residues were quantified using MS/MS spectral counts. Progress curves for the autophosphorylation of the individual juxtamembrane tyrosine residues (Y_{JM1} and Y_{JM2}) alone, as well as for their joint phosphorylation, $Y_{JM1+JM2}$, in the absence or presence of dimeric and preclustered ephrin ligand are colored as indicated.

(B) Progress curves for the autophosphorylation of the activation loop tyrosine residue, Y_{act}, in the semisynthetic receptor quantified using MS/MS spectral counts, in the absence (green) or presence of dimeric (red) and preclustered (blue) ephrin ligand. For each time point, the experimental data from three technical LC-MS/MS replicates performed on same amount of substrate was merged.

(C) Ligand-induced autophosphorylation of semisynthetic Eph receptors, wild-type (WT) and those with juxtamembrane tyrosine mutations ($Y_{JM1}F$, $Y_{JM2}F$ and $Y_{JM1+JM2}F$). Autoradiographs were quantified with PhosphorImager and are colored as indicated. Error bars represent the SD from three independent reactions. See also Figures S6 and S7.

addition to some of the questions addressed here, the analysis of the phosphorylation timelines of the individual Eph tyrosines can be extended further to investigate, for example, the differences in activation of the different promiscuous Eph family members in response to binding of different A and B class ligands (Bowden et al., 2009; Gale et al., 1996). The reported method should be general enough to be easily applicable to many other multidomain receptors allowing the production of large amounts of various functional cell-surface proteins for structural studies using X-ray crystallography and cryoelectron microscopy.

The generation of the semisynthetic EphA4 receptor provided a means to monitor the phosphorylation of its individual tyrosine residues during the ligand-induced kinase activation process. Our mass spectrometry experiments suggest that Eph receptors are activated upon ephrin binding via a sequential and ordered autophosphorylation process where Y_{JM2} is phosphorylated first, followed by Y_{JM1}, and, finally by Y_{act}. This is in contrast with observations for most other receptor kinases where the kinase activation loop is phosphorylated first. The most detailed such study involved the tyrosine kinase domain of FGF-Receptor-1, for which K. Anderson and colleagues reported a sequential phosphorylation mechanism where one of the two activation loop tyrosines (Y_{653}) is always the first tyrosine phosphorylated, while a juxtamembrane tyrosine is phosphorylated late in the activation process (Furdui et al., 2006; Lew et al., 2009). Similar kinase phosphorylation sequences, always beginning with activation loop phosphorylation, have also been suggested for the IR, IGFR, Tie2, and MuSK receptor kinases (discussed in detail in Furdui et al., 2006). The fact that in EphA4 the activation loop tyrosine is phosphorylated only after the juxtamembrane tyrosines underlies its unique signaling properties and the notion that the different receptor kinase families

can use different molecular mechanisms for kinase activation and inhibition. Importantly, in contrast to previous studies (Furdui et al., 2006; Lew et al., 2009), the reported here method allows the monitoring of ligand-induced kinase phosphorylation in a construct containing not only the intracellular, but also the extracellular (ligand binding) region of the receptors.

Our experiments reveal another unique Eph characteristic: the observed phosphorylation time-dependences suggest that the Eph kinase activity most closely correlates with the phosphorylation status of the juxtamembrane region and not that of the activation loop, as is the accepted view for most other characterized protein kinases (Hubbard and Till, 2000; Huse and Kuriyan, 2002; Schlessinger, 2000). Furthermore, our mutagenesis experiments show that the Eph kinase activity is primarily correlated with phosphorylation of Y_{JM2} and not of the adjacent Y_{JM1}. Interestingly, studies have shown that Eph signaling can be regulated by protein tyrosine phosphatases that specifically dephosphorylate Y_{JM2} (Shintani et al., 2006), further supporting an important role for this site in vivo. Our observations are also consistent with structural studies of the Eph kinase and juxtamembrane domains, showing that phosphorylation of the Eph activation loop does not significantly affect the architecture of the active site, whereas the conformation of the juxtamembrane region can alter the molecular dynamics of the kinase (Wiesner et al., 2006), and thus presumably its enzymatic activity. We are currently working on incorporating the 25 residue membrane sequence in the semisynthetic Ephs, which will allow for studying its precise role in the receptor activation mechanism, but we do not expect to see a change in the reported here order of individual tyrosine phosphorylation. The PDGF RTKs are also regulated by juxtamembrane region phosphorylation, but structural studies of c-Kit (Mol et al., 2004) and FLT3 (Griffith et al., 2004) suggest that there it is still the activation loop conformation that defines the kinase activity, while phosphorylation of the juxtamembrane regions removes a physical obstacle allowing the activation loop to adopt its active/open conformation for catalysis.

SIGNIFICANCE

While significant progress has been made in understanding how receptor tyrosine kinases regulate important cellular signaling pathways, a major challenge in conducting in vitro studies to elucidate the molecular details of the ligand-induced kinase activation is the lack of recombinant expression systems to produce large amounts of pure full-length proteins. Our work described here is aimed at overcoming this problem by development of a semisynthetic method to reconstitute functional Eph receptor tyrosine kinases in large amounts for structural and functional studies. Phosphoproteomics-based studies on such a semisynthetic Eph protein provide novel insight into the unique order of phosphorylation of individual phosphotyrosine residues in the ligand-induced kinase activation mechanism. The semisynthetic technique developed and described in this study could serve as a general method for reconstituting and studying the biochemical and structural details of receptor tyrosine kinases and other cell-surface receptors. Considering the importance of these molecules as drug targets in many diseases, our study should make significant contributions both in answering fundamental questions about signal transduction mechanisms and toward the discovery of novel therapeutics.

EXPERIMENTAL PROCEDURES

Protein Expression and Purification

The PCR amplified cDNA sequence corresponding to the ECD of human EphA4 (residues Glu30–Thr547) was cloned into a modified pAcGP67-B Baculovirus vector (BD PharMingen). The vector is under the control of the GP67 signal sequence and contains a C-terminal Fc (human IgG1 hinge and Fc regions) purification tag. The *Mxe* GyrA intein (198 amino acids) from the pTXB1 vector (New England Biolabs) was PCR amplified and fused in frame to the C terminus of EphA4 ECD between the ECD and the Fc purification tag. This intein with a C-terminal Asn → Ala mutation, promotes only the first step of protein splicing (Xu and Perler, 1996). The fusion construct (EphA4ECD-intein-Fc) was sequenced (Genewiz), and the recombinant baculovirus vector was cotransfected with BaculoGold DNA (BD PharMingen) in insect cells and expressed as previously described (Singla et al., 2008). The ectodomain of the human ephrin-A5 (residues 1–228) was cloned N-terminally to a thrombin cleavage site and the Fc region of IgG1 in a modified pcDNA3.1 vector (Invitrogen). The fusion construct (ephrin-A5-Fc) was constitutively expressed in a HEK293 (human embryonic kidney) cell line using the CD5 signal sequence as previously described (Barton et al., 2005). The secreted fusion proteins were extracted from the medium by affinity chromatography using Fast Flow Protein-A Sepharose (GE Healthcare). When required, the Fc tag was removed from ephrin-A5 by thrombin cleavage (1 U/mg of fusion protein) and it was purified by gel-filtration chromatography. The cDNA sequence corresponding to the juxtamembrane region and kinase domain of the human EphA3 (residues Gly569–Lys889) and EphA4 (residues Lys575–Ser896) receptors was PCR amplified and cloned C-terminally to a SUMO protease cleavage site in a modified pET SUMO vector (Invitrogen). The site-directed Ser → Cys mutation and insertion of the polyhistidine tag was performed with the QuickChange Mutagenesis Kit (Stratagene) at the N and C terminus of the EphA3/A4 ICD, respectively. The fusion constructs (His-SUMO-EphICD-His) were sequenced (Genewiz) and transformed into *E. coli* BL21-Gold (DE3) cells (Stratagene). Cells were grown in LB supplemented with kanamycin at 37°C to an OD_{600} of 0.5–0.6 and were induced overnight at 18°C and 1 mM IPTG. The proteins were purified on a HisTrap HP Nickel Sepharose column (GE Healthcare). The two-juxtamembrane tyrosine residues for EphA4 ICD were mutated to phenylalanine, individually and together, using the QuickChange Mutagenesis Kit (Stratagene). These three fusion constructs were then expressed and purified using the above protocol. The plasmid for YOP (YopH) phosphatase was provided by Dr. Markus A. Seeliger, it was expressed and purified as previously described (Seeliger et al., 2005).

Generation of EphA4 ECD α-Thioester and EphA3/A4 ICD with Reactive Cysteine

The purified EphA4ECD-intein-Fc fusion protein was bound to Protein-A Sepharose beads. The beads were re-suspended as 50% slurry into thiol cleavage buffer containing 100 mM HEPES (pH 7.5), 300 mM NaCl and 1 mM EDTA. Thiol agent MESNA was added at 50 mM and the slurry was incubated overnight at 4°C. The cleaved EphA4 ECD α-thioester was collected in the supernatant. The purified EphA3/A4 ICD were dialyzed into thiol cleavage buffer with 1 mM DTT and incubated with SUMO protease in a 1:400 (w/w) protease-to-protein ratio and 3 mM TCEP at 4°C for 1 hr, generating the reactive cysteine at the N terminus. The Eph ICD obtained after cleavage was loaded onto a Superdex-200 10/30 gel-filtration column (GE Healthcare) pre-equilibrated with a buffer containing 20 mM HEPES (pH 7.2) and 150 mM NaCl. The Eph ICDs were ligated to a synthetic peptide with a C-terminal α-thioester (synthesized by T.W.M.). The peptide (M-A-R-T-K-Q-T-A-R-K-S-T-G-G-K-A-P-R-K-Q-L-A-T-K-A-A-R-K-S-A-P-A) was dissolved in thiol cleavage buffer with 50 mM MESNA. The ligation reaction was performed by incubating overnight an excess of the peptide with freshly obtained reactive Eph ICD in ligation buffer containing 100 mM HEPES (pH 8.4) and 10 mM MESNA at 4°C.

Expressed Protein Ligation

The purified reactive EphA4 ECD α-thioester, obtained following thiol cleavage, and the reactive EphA4/A3 ICD, obtained after protease treatment, were concentrated (to millimolar range) and mixed in a 1:2 molar ratio. The ligation mixture was incubated for 48 hr at 4°C in ligation buffer containing 100 mM HEPES (pH 8.4), 50 mM MESNA, and 3 mM TCEP. The reaction was then loaded onto a Superdex-200 10/30 gel-filtration column (GE Healthcare) pre-equilibrated with a buffer containing 20 mM HEPES (pH 7.2) and 150 mM NaCl. The fractions corresponding to the semisynthetic Eph receptor and unligated Eph ECD α-thioester were pooled and buffer-exchanged into equilibration/wash buffer containing 50 mM Tris-HCl (pH 8.0), 30 mM imidazole, 300 mM NaCl, and 1 mM TCEP. The protein sample was loaded onto a HisTrap HP Nickel Sepharose column pre-equilibrated with the above buffer after which the column was washed with the same buffer. The bound protein was eluted with elution buffer containing 50 mM Tris-HCl (pH 8.0), 300 mM imidazole, 300 mM NaCl, and 1 mM TCEP. The eluted protein was loaded onto a Superdex-200 10/30 gel-filtration column pre-equilibrated as mentioned above. The fractions corresponding to the pure semisynthetic Eph receptor were pooled and stored at −80°C in a buffer containing 20 mM HEPES (pH 7.2), 150 mM NaCl, 1 mM TCEP, and 15% glycerol. The semisynthetic EphA4 receptor variants with the different juxtamembrane tyrosine mutations were obtained by the chemical ligation of the purified EphA4 ECD α-thioester with the respective EphA4 ICD mutant, using the above protocol.

Pull-Down and Gel-Filtration Ligand Binding Assays

The EphA4 ECD α-thioester, obtained following thiol cleavage and the semisynthetic Eph receptor, obtained after purification were incubated with Fc-tagged ephrin-A5 ligand in a 1:1 molar ratio. The pull-down experiments were performed as previously described (Singla et al., 2008). Gel-filtration studies for the EphA4 ECD α-thioester, purified ephrin-A5 ligand and the complex of both in a 1:1 molar ratio, were performed as previously described (Singla et al., 2008).

ELISA assay and Western Blotting

A nonradioactive kinase assay was performed using the ELISA-based protein tyrosine kinase assay kit (PTK101, Sigma). The unligated Eph ICD and the semisynthetic Eph receptor proteins in increasing concentration were incubated with Mg^{2+} and ATP for 30 min on wells coated with poly-Glu-Tyr peptide substrate. The phosphorylated peptide substrate was detected by ELISA using monoclonal HRP conjugated phosphotyrosine antibody and HRP chromogenic substrate. Optical density of each well was determined at 490 nm in a multiwell plate reader (Victor X5, PerkinElmer). Reagent preparation and detailed protocol were followed from the manufacturer's instructions. The semisynthetic Eph receptor was incubated with YOP phosphatase for 3 hr followed by overnight incubation with phosphatase inhibitor cocktail 2 (Sigma) at 4°C. Equal amounts of semisynthetic protein (10.4 nM) before and after phosphatase treatment were added to the substrate-coated wells in presence of $Mg^{2+}$and ATP. The kinase activity of both was monitored over a period of time using the ELISA assay described above. A synthetic peptide substrate [GG(EEEEY)$_{10}$EE] conjugated to biotin at its N terminus (Millipore), Mw = 7413 daltons, was used in the ELISA assay for the K_m measurements. To measure the K_m for the biotinylated peptide substrate, the concentrations of ATP, the unligated Eph ICD, and the semisynthetic Eph receptor proteins, were kept constant at 250 μM, 11 nM, and 10.4 nM, respectively, whereas the concentration of the peptide was varied from 0 to 25 μM. To measure the K_m for ATP, the concentrations of the biotinylated peptide substrate, the unligated Eph ICD, and the semisynthetic Eph receptor proteins, were kept constant at 5 μM, 11 nM, and 10.4 nM, respectively, whereas the ATP concentration was varied from 0 to 500 μM. The enzyme reactions were incubated for 5 min at 30°C and then quenched with 100 mM EDTA. Thereafter, the reaction mix was immobilized by binding to the preblocked streptavidin coated plates (Pierce). The phosphorylation of the biotinylated peptide substrate was visualized by ELISA using a phosphotyrosine monoclonal antibody conjugated to HRP and an ensuing chromogenic substrate reaction as described above. K_m values were calculated using the Michaelis-Menten equation using GraphPad Prism version 5.0a. For the western blot experiments, the semisynthetic Eph receptor was dephosphorylated by incubation with YOP phosphatase for 3 hr at 4°C and autophosphorylated back by simultaneous treatment with phosphatase inhibitor cocktail 2 (Sigma) for 2 hr and a buffer containing 30 mM HEPES (pH 7.5), 20 mM $MgCl_2$, and 10 mM ATP for 2 hr at 4°C. Protein samples were resolved on SDS-PAGE, electroblotted onto polyvinylidene difluoride membrane (BioRad), blocked with 2% fat free milk in TBST (0.5% Tween 20, 1.5 M NaCl in 100 mM Tris-HCl [pH 8.0]) and incubated overnight with the monoclonal phosphotyrosine antibody (4G10, Upstate Biotechnology). After rinsing with TBST, the membrane was incubated for 1 hr with the alkaline phosphatase (AP) conjugated secondary antibody (Promega). The AP was visualized with NBIT/BCIP substrate tablets (Roche).

In Vitro Kinase Assays

The disulfide-linked immunoglobulin Fc-tag results in formation of the dimeric ephrin-A5-Fc ligand. Ephrin-A5-Fc was clustered by overnight incubation with monoclonal anti-human IgG1 (anti-Fc) antibody (Jackson ImmunoResearch) in a 1:2 (w/w) ratio at 4°C to generate multimeric ephrin. For monitoring the ligand-induced kinase activity in the semisynthetic EphA4 receptor, equal quantity of the receptor was incubated with dimeric and pre-clustered ephrin-A5-Fc in a 1:1 molar ratio for 7 hr at 4°C, in the tyrosine kinase buffer containing 30 mM HEPES (pH 7.5), 20 mM $MgCl_2$, 1 mM $MnCl_2$, and 0.1 mg/ml bovine serum albumin. This was followed by incubation with YOP phosphatase for 5 hr at 4°C, and overnight incubation with phosphatase inhibitor cocktail 2 (Sigma) at 4°C. The reaction mixture was preincubated at 30°C for 5 min, and 0.3 mM ATP plus [γ^{32}-P] ATP (14.5 μCi) was added to start the reaction. The reaction mixture was incubated at 30°C and equal aliquots were withdrawn over a period of time for each of the three samples and terminated by adding Laemmli buffer. Reaction samples were resolved on SDS-PAGE, which were dried and exposed to a PhosphorImager screen (GE Healthcare). The [γ^{32}-P] ATP incorporation was quantified using ImageQuant software. The [γ^{32}-P] ATP incorporation in the semisynthetic EphA4 receptor with the juxtamembrane tyrosine mutations (Y_{JM1}F, Y_{JM2}F and $Y_{JM1+JM2}$F) on stimulation with dimeric ephrin-A5-Fc ligand, was also monitored using the radioactivity-based kinase assay described above. For measuring the stoichiometry of phosphate incorporation, a similar experimental set-up as described above was used. Reaction products were resolved on SDS-PAGE. Individual bands were excised, dissolved in 30% H_2O_2 (Sigma) and the incorporation of phosphate on tyrosine residues was measured using a liquid scintillation counter. For monitoring the kinase activity in the presence of the peptide Eph inhibitor, the peptide (synthesized by Biopeptide Inc.) was dissolved in peptide buffer containing 8% DMSO, 20 mM HEPES (pH 8.4), 150 mM NaCl, and 2 mM $MgCl_2$. The semisynthetic EphA4 receptor was incubated overnight with excess of the peptide inhibitor at 4°C along with two control reactions comprising of equal quantity of the semisynthetic receptor in peptide buffer. Dimeric ephrin-A5-Fc ligand was added to the receptor-peptide mix and to one of the control reactions. Using an experimental setup as described above the incorporation of labeled ATP was measured for the three samples.

Label Free Phosphoproteomics Analysis

Using a similar experimental set-up as described above with only 0.3 mM of unlabeled ATP for starting the reaction, nano-liquid chromatography coupled to mass spectrometry (nano-LC-MS/MS) analysis was performed to monitor the autophosphorylation of the semisynthetic Eph receptor by itself, and upon binding to dimeric and preclustered ephrin-A5-Fc ligand. The bands for the semisynthetic Eph protein were excised from the SDS-PAGE and digested overnight with trypsin as previously described (Sebastiaan Winkler et al., 2002). Resulting tryptic peptides were subjected to a micro-clean-up procedure as previously described (Erdjument-Bromage et al., 1998), and diluted with 0.1% formic acid. Analysis of the batch-purified pools was done using an LTQ OrbiTrap XL (Thermo Scientific) mass spectrometer with a nano-electrospray ion (ESI) source coupled to an Eksigent nano-LC system (Eksigent Technologies). For each time point, three technical LC-MS/MS replicates were performed on same amount of substrate and the experimental data was merged before database searching. Initial protein/peptide identification from LC-MS/MS data was done using the Mascot search engine (Matrix Science, version 2.2.04; www.matrixscience.com), the NCBI (National Library of Medicine, NIH), and IPI (International Protein Index, EBI, Hinxton, UK) databases. Two missed tryptic cleavage sites were allowed; precursor ion mass tolerance = 10 ppm, fragment ion mass tolerance = 0.8 Da; peptide variable modifications were allowed for methionine oxide, cysteine acrylamide, and

phosphorylation at tyrosine amino acids. MudPit scoring was typically applied using significance threshold score $p < 0.01$. Identified peptide counts (spectral counts) and percent sequence coverage were then imported to Scaffold Proteome Software (www.proteomesoftware.com, version 2.05) for further analysis. Since we started with the same amount of protein, the % sequence coverage indicating the percentage of the entire length of the protein that was represented by all the identified tryptic peptides combined was very similar for each time point. For relative quantification based on number of MS/MS spectra (Asara et al., 2008) (spectral count) collected, we utilized peptide identification probability at 90% setting to extract the spectral count for each of the phosphotyrosine containing peptides spanning Y_{JM1}, Y_{JM2} and Y_{act} sites.

SUPPLEMENTAL INFORMATION

Supplemental Information includes seven figures and can be found with this article online at doi:10.1016/j.chembiol.2011.01.011.

ACKNOWLEDGMENTS

We thank Dr. Parag Patwardhan (Merilyn Resh lab, MSKCC) for help with the radioactive kinase assays. We thank Isabelle Harroch for help with mass spectrometric analysis. We thank Drs. W. Todd Miller, Anant K. Menon, and Morgan Huse for helpful discussion. We thank Dr. Alexander Antipenko for the custom-made baculovirus expression vector (pMA-152). This work was supported by the National Institutes of Health grant NS38486 (to D.B.N.) and the NCI Cancer Center support grant P30 CA08748 (to H.E-B.).

Received: September 2, 2010
Revised: December 19, 2010
Accepted: January 5, 2011
Published: March 24, 2011

REFERENCES

Asara, J.M., Christofk, H.R., Freimark, L.M., and Cantley, L.C. (2008). A label-free quantification method by MS/MS TIC compared to SILAC and spectral counting in a proteomics screen. Proteomics *8*, 994–999.

Barton, W.A., Tzvetkova, D., and Nikolov, D.B. (2005). Structure of the angiopoietin-2 receptor binding domain and identification of surfaces involved in Tie2 recognition. Structure *13*, 825–832.

Binns, K.L., Taylor, P.P., Sicheri, F., Pawson, T., and Holland, S.J. (2000). Phosphorylation of tyrosine residues in the kinase domain and juxtamembrane region regulates the biological and catalytic activities of Eph receptors. Mol. Cell. Biol. *20*, 4791–4805.

Black, D.S., and Bliska, J.B. (1997). Identification of p130Cas as a substrate of Yersinia YopH (Yop51), a bacterial protein tyrosine phosphatase that translocates into mammalian cells and targets focal adhesions. EMBO J. *16*, 2730–2744.

Bowden, T.A., Aricescu, A.R., Nettleship, J.E., Siebold, C., Rahman-Huq, N., Owens, R.J., Stuart, D.I., and Jones, E.Y. (2009). Structural plasticity of eph receptor A4 facilitates cross-class ephrin signaling. Structure *17*, 1386–1397.

Boyd, A.W., Ward, L.D., Wicks, I.P., Simpson, R.J., Salvaris, E., Wilks, A., Welch, K., Loudovaris, M., Rockman, S., and Busmanis, I. (1992). Isolation and characterization of a novel receptor-type protein tyrosine kinase (hek) from a human pre-B cell line. J. Biol. Chem. *267*, 3262–3267.

Butt, T.R., Edavettal, S.C., Hall, J.P., and Mattern, M.R. (2005). SUMO fusion technology for difficult-to-express proteins. Protein Expr. Purif. *43*, 1–9.

Chumley, M.J., Catchpole, T., Silvany, R.E., Kernie, S.G., and Henkemeyer, M. (2007). EphB receptors regulate stem/progenitor cell proliferation, migration, and polarity during hippocampal neurogenesis. J. Neurosci. *27*, 13481–13490.

Davis, S., Gale, N.W., Aldrich, T.H., Maisonpierre, P.C., Lhotak, V., Pawson, T., Goldfarb, M., and Yancopoulos, G.D. (1994). Ligands for EPH-related receptor tyrosine kinases that require membrane attachment or clustering for activity. Science *266*, 816–819.

Davis, T.L., Walker, J.R., Loppnau, P., Butler-Cole, C., Allali-Hassani, A., and Dhe-Paganon, S. (2008). Autoregulation by the juxtamembrane region of the human ephrin receptor tyrosine kinase A3 (EphA3). Structure *16*, 873–884.

Dawson, P.E., Muir, T.W., Clark-Lewis, I., and Kent, S.B. (1994). Synthesis of proteins by native chemical ligation. Science *266*, 776–779.

Dottori, M., Down, M., Huttmann, A., Fitzpatrick, D.R., and Boyd, A.W. (1999). Cloning and characterization of EphA3 (Hek) gene promoter: DNA methylation regulates expression in hematopoietic tumor cells. Blood *94*, 2477–2486.

Drew, D., Froderberg, L., Baars, L., and de Gier, J.W. (2003). Assembly and overexpression of membrane proteins in Escherichia coli. Biochim. Biophys. Acta *1610*, 3–10.

Eph Nomenclature Committee. (1997). Unified nomenclature for Eph family receptors and their ligands, the ephrins. Cell *90*, 403–404.

Erdjument-Bromage, H., Lui, M., Lacomis, L., Grewal, A., Annan, R.S., McNulty, D.E., Carr, S.A., and Tempst, P. (1998). Examination of micro-tip reversed-phase liquid chromatographic extraction of peptide pools for mass spectrometric analysis. J. Chromatogr. A *826*, 167–181.

Furdui, C.M., Lew, E.D., Schlessinger, J., and Anderson, K.S. (2006). Autophosphorylation of FGFR1 kinase is mediated by a sequential and precisely ordered reaction. Mol. Cell *21*, 711–717.

Gale, N.W., Holland, S.J., Valenzuela, D.M., Flenniken, A., Pan, L., Ryan, T.E., Henkemeyer, M., Strebhardt, K., Hirai, H., Wilkinson, D.G., et al. (1996). Eph receptors and ligands comprise two major specificity subclasses and are reciprocally compartmentalized during embryogenesis. Neuron *17*, 9–19.

Griffith, J., Black, J., Faerman, C., Swenson, L., Wynn, M., Lu, F., Lippke, J., and Saxena, K. (2004). The structural basis for autoinhibition of FLT3 by the juxtamembrane domain. Mol. Cell *13*, 169–178.

Guan, K.L., and Dixon, J.E. (1990). Protein tyrosine phosphatase activity of an essential virulence determinant in Yersinia. Science *249*, 553–556.

Himanen, J.P., and Nikolov, D.B. (2003). Eph signaling: a structural view. Trends Neurosci. *26*, 46–51.

Himanen, J.P., Rajashankar, K.R., Lackmann, M., Cowan, C.A., Henkemeyer, M., and Nikolov, D.B. (2001). Crystal structure of an Eph receptor-ephrin complex. Nature *414*, 933–938.

Himanen, J.P., Saha, N., and Nikolov, D.B. (2007). Cell-cell signaling via Eph receptors and ephrins. Curr. Opin. Cell Biol. *19*, 534–542.

Himanen, J.P., Yermekbayeva, L., Janes, P.W., Walker, J.R., Xu, K., Atapattu, L., Rajashankar, K.R., Mensinga, A., Lackmann, M., Nikolov, D.B., et al. (2010). Architecture of Eph receptor clusters. Proc. Natl. Acad. Sci. USA *107*, 10860–10865.

Hubbard, S.R., and Till, J.H. (2000). Protein tyrosine kinase structure and function. Annu. Rev. Biochem. *69*, 373–398.

Huse, M., and Kuriyan, J. (2002). The conformational plasticity of protein kinases. Cell *109*, 275–282.

Jiang, Y., Lee, A., Chen, J., Ruta, V., Cadene, M., Chait, B.T., and MacKinnon, R. (2003). X-ray structure of a voltage-dependent K+ channel. Nature *423*, 33–41.

Kawate, T., and Gouaux, E. (2006). Fluorescence-detection size-exclusion chromatography for precrystallization screening of integral membrane proteins. Structure *14*, 673–681.

Kullander, K., and Klein, R. (2002). Mechanisms and functions of Eph and ephrin signalling. Nat. Rev. Mol. Cell Biol. *3*, 475–486.

Lackmann, M., and Boyd, A.W. (2008). Eph, a protein family coming of age: more confusion, insight, or complexity? Sci. Signal. *1*, re2.

Lawrenson, I.D., Wimmer-Kleikamp, S.H., Lock, P., Schoenwaelder, S.M., Down, M., Boyd, A.W., Alewood, P.F., and Lackmann, M. (2002). Ephrin-A5 induces rounding, blebbing and de-adhesion of EphA3-expressing 293T and melanoma cells by CrkII and Rho-mediated signalling. J. Cell Sci. *115*, 1059–1072.

Lew, E.D., Furdui, C.M., Anderson, K.S., and Schlessinger, J. (2009). The precise sequence of FGF receptor autophosphorylation is kinetically driven and is disrupted by oncogenic mutations. Sci. Signal. *2*, ra6.

Li, S.J., and Hochstrasser, M. (1999). A new protease required for cell-cycle progression in yeast. Nature *398*, 246–251.

Marblestone, J.G., Edavettal, S.C., Lim, Y., Lim, P., Zuo, X., and Butt, T.R. (2006). Comparison of SUMO fusion technology with traditional gene fusion systems: enhanced expression and solubility with SUMO. Protein Sci. *15*, 182–189.

Mizushima, S., and Nagata, S. (1990). pEF-BOS, a powerful mammalian expression vector. Nucleic Acids Res. *18*, 5322.

Mol, C.D., Dougan, D.R., Schneider, T.R., Skene, R.J., Kraus, M.L., Scheibe, D.N., Snell, G.P., Zou, H., Sang, B.C., and Wilson, K.P. (2004). Structural basis for the autoinhibition and STI-571 inhibition of c-Kit tyrosine kinase. J. Biol. Chem. *279*, 31655–31663.

Mossessova, E., and Lima, C.D. (2000). Ulp1-SUMO crystal structure and genetic analysis reveal conserved interactions and a regulatory element essential for cell growth in yeast. Mol. Cell *5*, 865–876.

Muir, T.W. (2003). Semisynthesis of proteins by expressed protein ligation. Annu. Rev. Biochem. *72*, 249–289.

Muir, T.W., Sondhi, D., and Cole, P.A. (1998). Expressed protein ligation: a general method for protein engineering. Proc. Natl. Acad. Sci. USA *95*, 6705–6710.

Muller, S., Hoege, C., Pyrowolakis, G., and Jentsch, S. (2001). SUMO, ubiquitin's mysterious cousin. Nat. Rev. Mol. Cell Biol. *2*, 202–210.

Murai, K.K., Nguyen, L.N., Koolpe, M., McLennan, R., Krull, C.E., and Pasquale, E.B. (2003). Targeting the EphA4 receptor in the nervous system with biologically active peptides. Mol. Cell. Neurosci. *24*, 1000–1011.

Muralidharan, V., and Muir, T.W. (2006). Protein ligation: an enabling technology for the biophysical analysis of proteins. Nat. Methods *3*, 429–438.

Pasquale, E.B. (2005). Eph receptor signalling casts a wide net on cell behaviour. Nat. Rev. Mol. Cell Biol. *6*, 462–475.

Saitoh, H., Pu, R.T., and Dasso, M. (1997). SUMO-1: wrestling with a new ubiquitin-related modifier. Trends Biochem. Sci. *22*, 374–376.

Schlessinger, J. (2000). Cell signaling by receptor tyrosine kinases. Cell *103*, 211–225.

Schwarzer, D., and Cole, P.A. (2005). Protein semisynthesis and expressed protein ligation: chasing a protein's tail. Curr. Opin. Chem. Biol. *9*, 561–569.

Sebastiaan Winkler, G., Lacomis, L., Philip, J., Erdjument-Bromage, H., Svejstrup, J.Q., and Tempst, P. (2002). Isolation and mass spectrometry of transcription factor complexes. Methods *26*, 260–269.

Seeliger, M.A., Young, M., Henderson, M.N., Pellicena, P., King, D.S., Falick, A.M., and Kuriyan, J. (2005). High yield bacterial expression of active c-Abl and c-Src tyrosine kinases. Protein Sci. *14*, 3135–3139.

Severinov, K., and Muir, T.W. (1998). Expressed protein ligation, a novel method for studying protein-protein interactions in transcription. J. Biol. Chem. *273*, 16205–16209.

Shintani, T., Ihara, M., Sakuta, H., Takahashi, H., Watakabe, I., and Noda, M. (2006). Eph receptors are negatively controlled by protein tyrosine phosphatase receptor type O. Nat. Neurosci. *9*, 761–769.

Singla, N., Himanen, J.P., Muir, T.W., and Nikolov, D.B. (2008). Toward the semisynthesis of multidomain transmembrane receptors: modification of Eph tyrosine kinases. Protein Sci. *17*, 1740–1747.

Valiyaveetil, F.I., MacKinnon, R., and Muir, T.W. (2002). Semisynthesis and folding of the potassium channel KcsA. J. Am. Chem. Soc. *124*, 9113–9120.

Wallin, E., and von Heijne, G. (1998). Genome-wide analysis of integral membrane proteins from eubacterial, archaean, and eukaryotic organisms. Protein Sci. *7*, 1029–1038.

Wiesner, S., Wybenga-Groot, L.E., Warner, N., Lin, H., Pawson, T., Forman-Kay, J.D., and Sicheri, F. (2006). A change in conformational dynamics underlies the activation of Eph receptor tyrosine kinases. EMBO J. *25*, 4686–4696.

Wybenga-Groot, L.E., Baskin, B., Ong, S.H., Tong, J., Pawson, T., and Sicheri, F. (2001). Structural basis for autoinhibition of the Ephb2 receptor tyrosine kinase by the unphosphorylated juxtamembrane region. Cell *106*, 745–757.

Xu, M.Q., and Perler, F.B. (1996). The mechanism of protein splicing and its modulation by mutation. EMBO J. *15*, 5146–5153.

Zhang, Z.Y., Clemens, J.C., Schubert, H.L., Stuckey, J.A., Fischer, M.W., Hume, D.M., Saper, M.A., and Dixon, J.E. (1992). Expression, purification, and physicochemical characterization of a recombinant Yersinia protein tyrosine phosphatase. J. Biol. Chem. *267*, 23759–23766.